COMPDYN 2015
5th ECCOMAS Thematic Conference on
Computational Methods in Structural Dynamics and Earthquake Engineering
M. Papadrakakis, V. Papadopoulos, V. Plevris (eds.)
Crete Island, Greece, 25–27 May 2015

EXPERIMENTAL VERIFICATION OF DAMAGE LOCATION TECHNIQUES FOR FRAME STRUCTURES ASSEMBLED USING BOLTED CONNECTIONS

Bartlomiej Blachowski[1], Andrzej Swiercz[1], and Nikos Pnevmatikos[2]

[1] Institute of Fundamental Technological Research
Polish Academy of Sciences
Warsaw, Poland
bblach@ippt.pan.pl, aswiercz@ippt.pan.pl

[2] Technological Educational Institution of Athens
Department of Civil Engineering, Surveying and Geoinformatics
Athens, Greece
pnevma@teiath.gr

Keywords: bolted lap connection, frame structure, experimental modal analysis, damage location.

Abstract. *This work is focused on experimental verification of existing techniques for localization of a loosened bolted connection. To this end, a laboratory-scale 2-meter-long steel frame is used. The structure consists of 11 steel beams forming a four-bay frame, which is subjected to impact loads using a modal hammer. The accelerations are measured at 20 different locations on the frame, including joints and beam elements. Two states of the structure are considered: a healthy and a damaged one. The damage is introduced by means of loosening two out of three bolts at one of the frame connections. Experimental modal analysis reveals that the loosened bolts in the connection cause a shift only in some of the frame's natural frequencies, while the others remain insensitive to the damage.*

1 INTRODUCTION

Many papers devoted to damage localization methods deal with damage scenarios in the form of reduced beam cross sections [1,2], cracks [3,4], reduced plate thickness or plate cracks [5,6]. In reality, however, many structural failures start from damages which occur at connections. One of examples is the loosening of one or more bolts in bolted lap joints. The work on damage identification of bolted connections in a steel frame by Yang et al. [7] is a representative study. The method of artificial neural networks was adopted for damage detection in truss bridge joints, Mehrjoo et al. [8]. The influence of joint stiffness on global modes of structures was presented in the work of Blachowski and Gutkowski [9]. A damage detection approach to bolted flange joints in pipelines was presented by Razi et al. [10].

Another tool for damage detection is the wavelet-based method, as shown in the works of Staszewski, [11] and Newland, [12]. An exemplary application of the wavelet transform in to damage detection in a steel frame with plastic hinges has been presented by Pnevmatikos [13].

This work is focused on experimental verification of existing techniques for localization of a loosened bolted connection. To this end, a laboratory-scale steel frame is used. The work is divided into two parts: the first one is related to the performed experimental study and the second one to the computational techniques for damage localization. The computational techniques includes: modal assurance criterion, frequency response function (FRF), and wavelets transformation. In order to localize a damaged bolted connection a new measure is introduced called Damage Connection Index. This is essentially the sum of absolute values of the difference in angles of rotation at the given bolted connection.

2 TESTED STRUCTURE

2.1 Overview of the experimental stand

For the purpose of experimental verification of damage locating methods, a simple frame structure shown in Figure 1(a) is used. The structure is modular and consists of four square bays, each 0.51m high and wide. Each bay is composed of steel elements of equal length with a rectangular cross-section of 8 by 80 mm. The total number of elements is 11 and the total length of the structure is 2.04 m. The structure is supported at the outermost nodes, preventing both translational and rotational displacements. The connections between elements are realized by means of rigid connector elements (nodes) and allen bolts (6mm diameter), which are shown in Figure 1(c) and 1(b), respectively. Each such connection is designed to use 3 bolts screwed into threaded holes in the elements. The original structure (without modification) is referred here as the *reference structure* and the responses (accelerations) collected in the test I are called the *reference responses*.

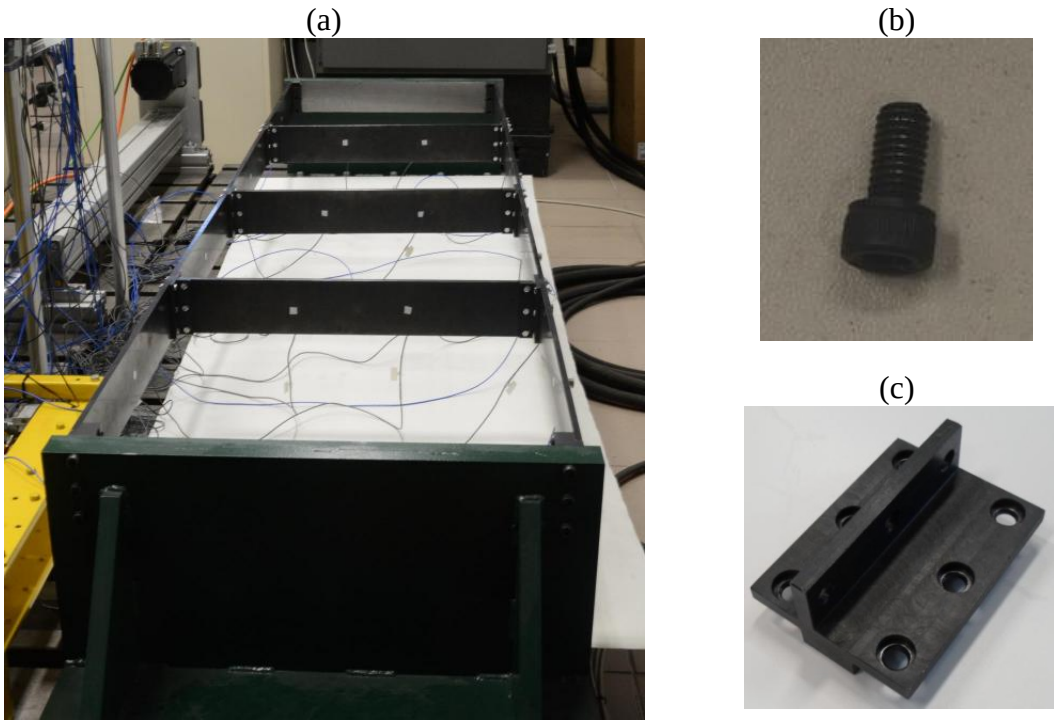

Figure 1: (a) The examined frame structure, (b) an allen bolt used for the element-node connections, (c) a connector element (node).

A modification is introduced to node 5 and element 10 (see Figure 2). The modification of the connection consists in removing 2 bolts (bottom and upper), leaving the middle one. In contrast to the reference structure and the reference responses, we will use here the notions of *modified structure* and *modified responses*, respectively. The modified responses gathered during the measurement session are denoted as test II.

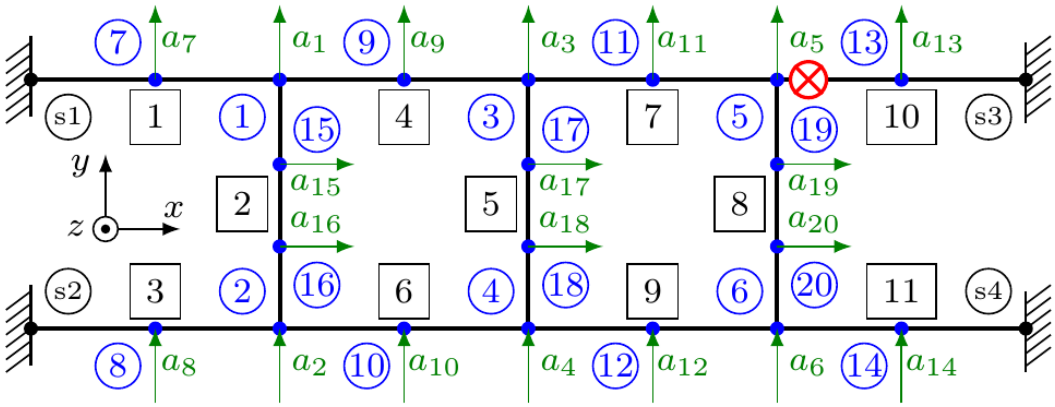

Figure 2: Scheme of the tested frame structure. Notation: *s1-s4* fixed nodal points, 1-20 (in circles) nodal points, 1-11 (in boxes) element numbers, a_1-a_{20} measured accelerations at nodal points. The location of the loosened bolted connection in shown in red.

2.2 Instrumentation & measurement procedure

Vibrations of the reference and modified structures were measured using 20 single axis accelerometers arranged as presented in Figure 2. All transducers were located in the mid-plane of the structure: at the centers of elements (the main axis parallel to the X-axis), one-third and two-thirds of the elements' lengths (the main axis parallel to the Y-axis). The structural vibrations were induced using a modal hammer with an embedded force sensor. The applied plastic tip allowed for covering the excitation frequency range of up to 1 kHz. The measurements were divided into two scenarios: for test I (for the reference structure) and test II (for the modified structure). For each scenario, two trial series were performed. The single trial serie consisted of tests with the impact loading applied at the selected set of nodes: 2, 5, 8, 10, 11, 13, 16, 17, 19 (cf. Figure 2). For every single test, 20 acceleration responses and one impulse force from the modal hammer were collected.

In all, 21 signals in the time domain (recording time 40 s) with a sampling rate of 32 kHz were collected during the single trial serie. For the collected signals, the Frequency Response Functions (FRF's) were computed. Finally, based on FRF's, a classical modal analysis was conducted leading to the estimation of modal parameters for the reference and modified structures. The measurement data were collected using the PULSE system (*Bruel&Kjaer*) and the modal analysis was performed utilizing the PolyMAX method implemented in the commercial software LMS Test.Lab (*Siemens PLM Software*).

3 ANALYSIS OF MODE SHAPES AND FREQUENCIES

For the collected data, the classical modal analysis was performed aimed at determination of modal parameters of the above-mentioned two states (reference and modified) of the structure. Further considerations are focused on resonant frequencies and modal shapes, since damping ratios are generally very low (do not exceed 0.3%) with very little variations.

The identified frequencies for the reference and modified structures are presented in Table 1. Moreover, Table 1 contains absolute and relative frequency differences and modal assurance criterion (MAC) values computed for each corresponding pair of frequencies. At first glance, the corresponding resonant frequencies are close to each other; however, modes 11 and 12 vary from Test I to Test II (cf. Figure 3). This presents the sensitivity of the modal frequencies to the introduced nodal modification. As presented in Figure 3, the absolute difference for the 13^{th} modal frequency is very low, but the corresponding MAC value presented in Table 1 is also relatively low. This means, that the 13^{th} modal shape is sensitive to the structural modification, while the corresponding modal frequencies obtained for the reference and modified structures are similar. Only the 12^{th} mode is sensitive with respect to both the modal shape and the modal frequency.

Mode no.	Test I (intact structure) frequency [Hz]	Test II (modified structure) frequency [Hz]	Absolute difference [Hz]	Relative difference [100%]	MAC value [100%]
	f_i^I	f_i^{II}	$f_i^I - f_i^{II}$	$\frac{f_i^I - f_i^{II}}{f_i^I}$	$\frac{((\Phi_i^I)^T \Phi_i^{II})^2}{\lvert\Phi_i^I\rvert^2 \lvert\Phi_i^{II}\rvert^2}$
1	12.33	12.29	0.04	0.34	77.6
2	26.65	26.58	0.07	0.27	98.8
3	40.53	40.35	0.18	0.45	98.8
4	78.38	78.23	0.15	0.19	100.0
5	97.14	97.06	0.09	0.09	100.0
6	109.50	109.44	0.06	0.05	100.0
7	115.14	115.13	0.01	0.01	100.0
8	138.32	138.20	0.12	0.09	100.0
9	161.37	161.37	−0.01	−0.00	97.8
10	162.30	162.30	0.00	0.00	98.6
11	169.00	166.44	2.57	1.52	98.1
12	173.24	170.23	3.01	1.74	89.1
13	173.81	173.68	0.13	0.08	76.6
14	207.08	206.25	0.83	0.40	99.8
15	305.37	304.80	0.56	0.19	99.9
16	346.09	345.59	0.50	0.15	99.9
17	373.81	373.65	0.16	0.04	100.0

Table 1: Resonant frequencies, their differences and MAC values of the (reference and modified) structure obtained from experimental tests.

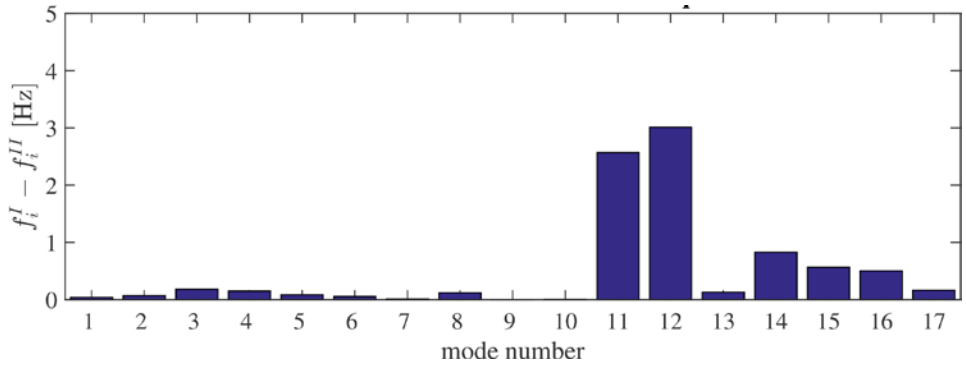

Figure 3: Absolute differences between the modal frequencies of the reference and modified structure.

In Figures 4 and 5 are shown the frequency response functions (FRFs) for the frequency band 100-200 Hz obtained for two states of the structure. In the first case, the collected response (output) at node 8 is referred to the excitation force applied at the same nodal point (cf. Figure 2). For tests I and II, two trials were executed revealing frequency shifting. A similar effect was observed for the 13th nodal point, presented in Figure 5.

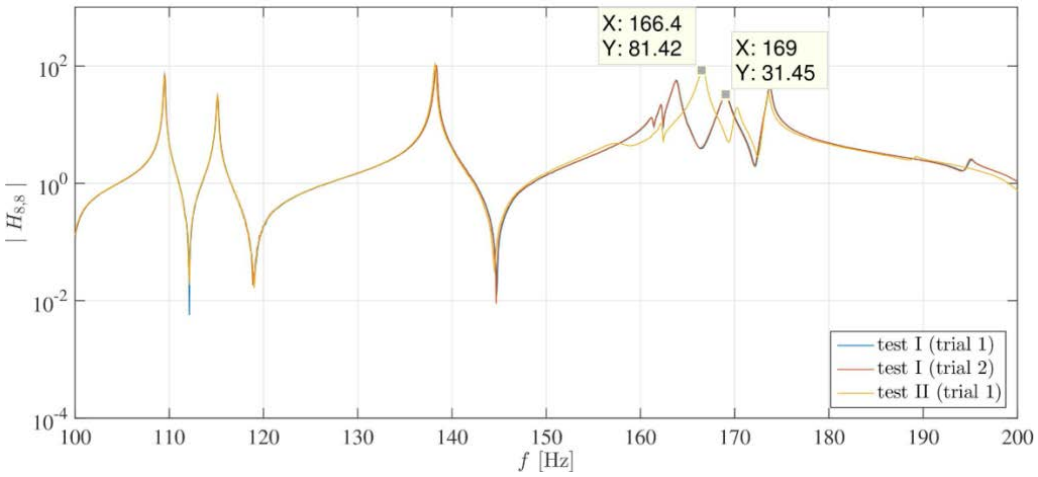

Figure 4: Comparison of frequency response functions (FRFs) of the reference (test I) and modified (test II) structures obtained for the excitation at nodal point no. 8.

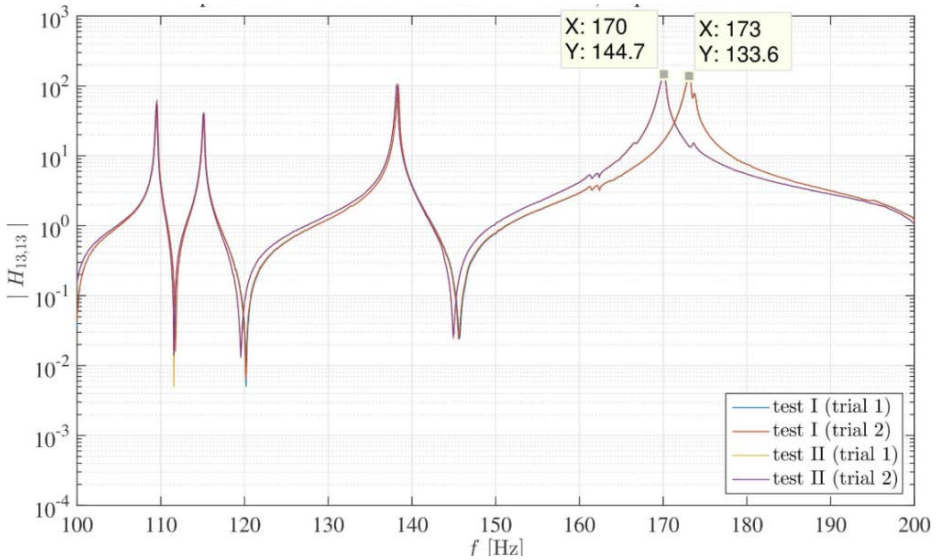

Figure 5: Comparison of frequency response functions (FRFs) of the reference (test I) and modified (test II) structures obtained for the excitation at nodal point no. 13.

A comparison of selected modal shapes of the two states of the structure is presented in Figure 6. Figure 6(a) shows using the example of the 8th mode that most identified modal shapes do not exhibit any substantial changes. Only for three modes, 11th, 12th and 13th the differences are significant (cf. Figures 6(b), 6(c), 6(d)).

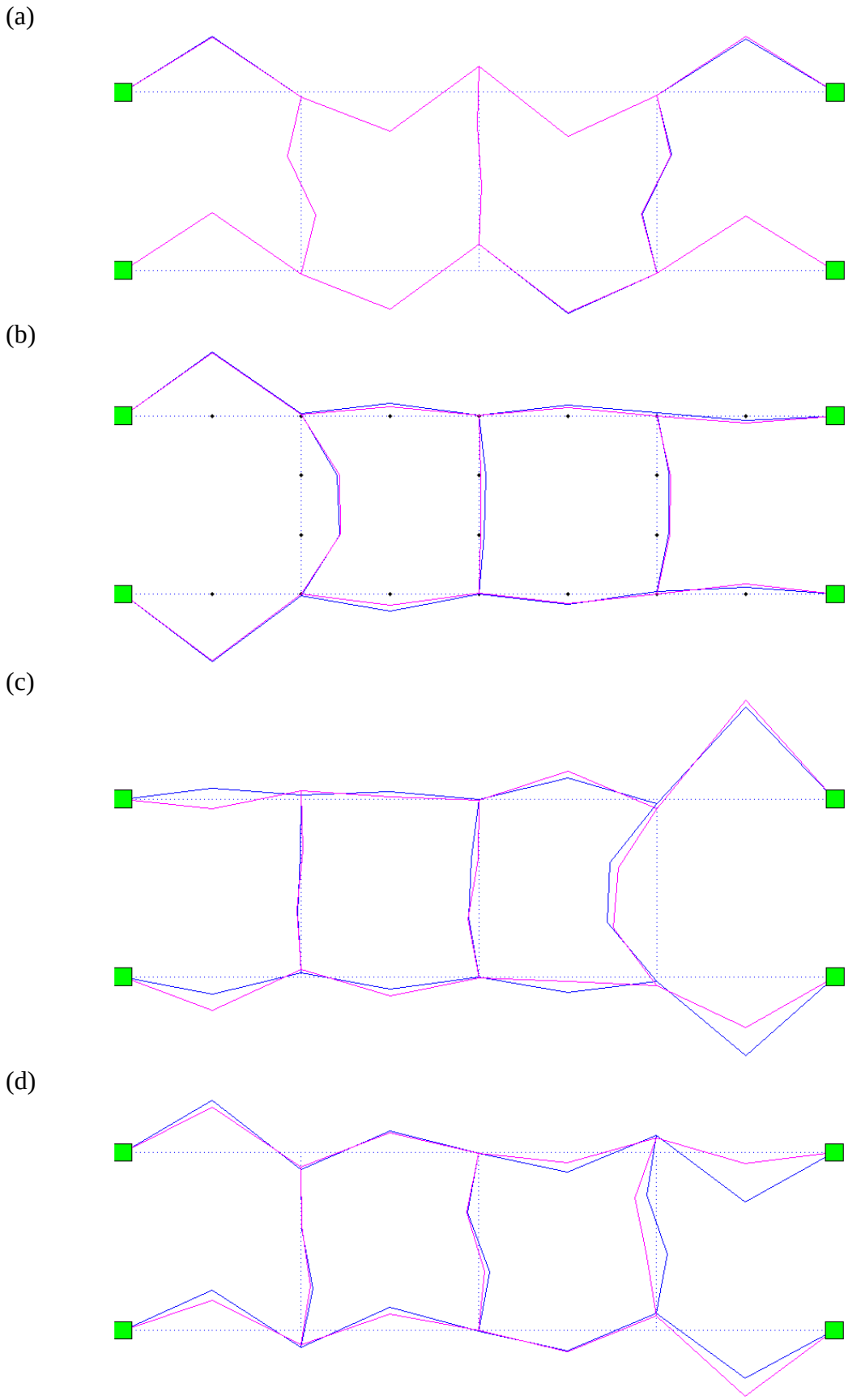

Figure 6: Comparison of modal shapes obtained for the reference (red lines) and modified (blue lines) structures: (a) mode shape no. 8, (b) mode shape no. 11, (c) mode shape no. 12, (d) mode shape no. 13.

The loosened bolted connection causes changes to the *i*-th modal vector of the frame. Let us define the difference in the angles of rotation $\Delta\alpha_j^{(i)}$ for *i*-th modal shape and *j*-th connection:

$$\Delta\alpha_j^{(i)} = \sum_{k=1}^{m}\left[T_{j,k}(\Phi_{i,k} - \widehat{\Phi}_{i,k})\right] \tag{1a}$$

or in matrix notation

$$\Delta\boldsymbol{\alpha}^{(i)} = \boldsymbol{T}\left(\boldsymbol{\Phi}_i - \widehat{\boldsymbol{\Phi}}_i\right) \tag{1b}$$

where m is the number of measured DOFs, $\boldsymbol{\Phi}_i$ and $\widehat{\boldsymbol{\Phi}}_i$ are the *i*-th modal vectors of the healthy and damaged structures, $\boldsymbol{T}$ is a matrix transforming modal displacements into angles of rotation. For each mode shape, the dimension of the vector $\Delta\boldsymbol{\alpha}^{(i)}$ is equal to 18, since we consider 18 connections located as shown in Figure 7. For example, the computation of the angle of rotation $\Delta\alpha_2^{(i)}$ (for connection no. 2) is performed based on the first and ninth (cf. Figure 2) components of modal vectors $\boldsymbol{\Phi}_i$ and $\widehat{\boldsymbol{\Phi}}_i$ as follows:

$$\Delta\alpha_2^{(i)} = \frac{2}{L_4}\left(\Phi_{i,9} - \Phi_{i,1}\right) - \frac{2}{L_4}\left(\widehat{\Phi}_{i,9} - \widehat{\Phi}_{i,1}\right) \tag{2}$$

In the above equation, L_4 denotes the length of the element no. 4, and $\Phi_{i,1}$, $\Phi_{i,9}$ and $\widehat{\Phi}_{i,1}$, $\widehat{\Phi}_{i,9}$ are the first and ninth components of the *i*-th modal vectors $\boldsymbol{\Phi}_i$, $\widehat{\boldsymbol{\Phi}}_i$, respectively.
Thus, in the second row of the transformation matrix $\boldsymbol{T}$ only two components are non-zero, i.e.

$$T_{2,1} = -\frac{2}{L_4}, \quad T_{2,9} = \frac{2}{L_4}$$

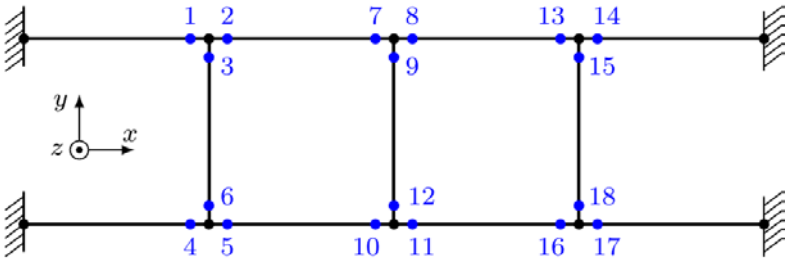

Figure 7: Localization of the considered nodal connections.

Carrying out calculations for all identified modal vectors we get the rectangular-shaped matrix $\Delta\boldsymbol{\alpha}$ with the dimensions 18x17. For the assessment of the severity of damage in an individual connection, the Damage Connection Index (DCI) is proposed:

$$a_j = \sum_i |\Delta\boldsymbol{\alpha}^{(i)}|^n \tag{2}$$

where a_j is the sum of the differences in angles of rotation over all identified modes, and n is a parameter. Figure 8 presents the a_j values for each bolted connection as marked in Figure 7.

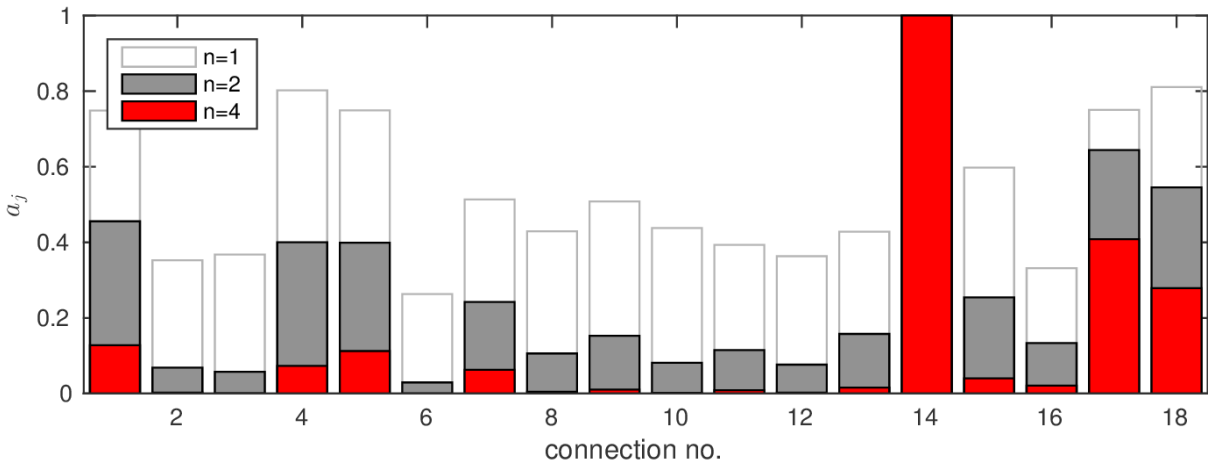

Figure 8: Values of the DCI for different values of the exponent *n*.

Depending on the assumed parameter *n*, the values of the DCI differ significantly. For *n=1* the DCI values are comparable; however, an extreme value is obtained for the connection no.14. When increasing the parameter *n*, the observed differences between the DCI values became more substantial. For *n=2* and *n=4*, the highest value of the vector $\boldsymbol{a}$ is reached for *j=14* and this clearly indicates the localization of the introduced modification.

4 WAVELET TRANSFOM ANALYSIS

Wavelet analysis provides a powerful tool to characterize local features of a signal. Unlike the Fourier transform, where the function used as the basis of decomposition is always a sinusoidal wave, other basis functions can be selected for the wavelet shape according to the features of the signal. The basis function in wavelet analysis is defined by two parameters: scale and translation. These properties lead to a multi-resolution representation for non-stationary signals.

The continuous wavelet transform of a signal $f(t)$ is defined as:

$$f(a,b) = \frac{1}{\sqrt{a}} \int_{-\infty}^{\infty} f(t) \overline{\Psi}\left(\frac{t-b}{a}\right) dt \tag{3}$$

where *a*, *b* are the scale and translation parameters respectively and $\overline{\Psi}$ denotes the complex conjugate of Ψ. The functions $\Psi(t,a,b)$ are called wavelets. They are dilated and translated versions of the mother wavelet $\Psi(t)$. There are a lot of types of wavelet functions $\Psi(t)$; Figure 9 shows the Haar wavelet function which was used in the analysis in this paper. The Haar wavelet's mother wavelet function $\Psi(t)$ can be described as:

$$\Psi(t) = \begin{cases} 1 & 0 \le t < \frac{1}{2} \\ -1 & \frac{1}{2} \le t < 1 \\ 0 & \text{otherwise} \end{cases} \tag{4}$$

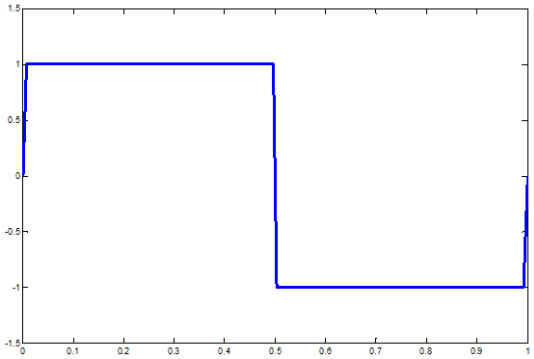

Figure 9: Continuous wavelet Haar function $\Psi(t)$.

An application of continuous wavelet analysis to damage detection in a frame structure subjected to impact loading was also performed. Wavelet analysis was made of the obtained response acceleration data collected in the test I, corresponding to the reference structure, and those collected in the test II, corresponding to the modified structure. The Haar wavelet function was used in the analysis of the output signals. The results of the wavelet analysis of the reference and modified structures are shown in Figure 10. In this figure, the magnitude versus scale (frequency) and time is presented for the reference, Figure 10 (a), and the modified structure Figure 10 (b).

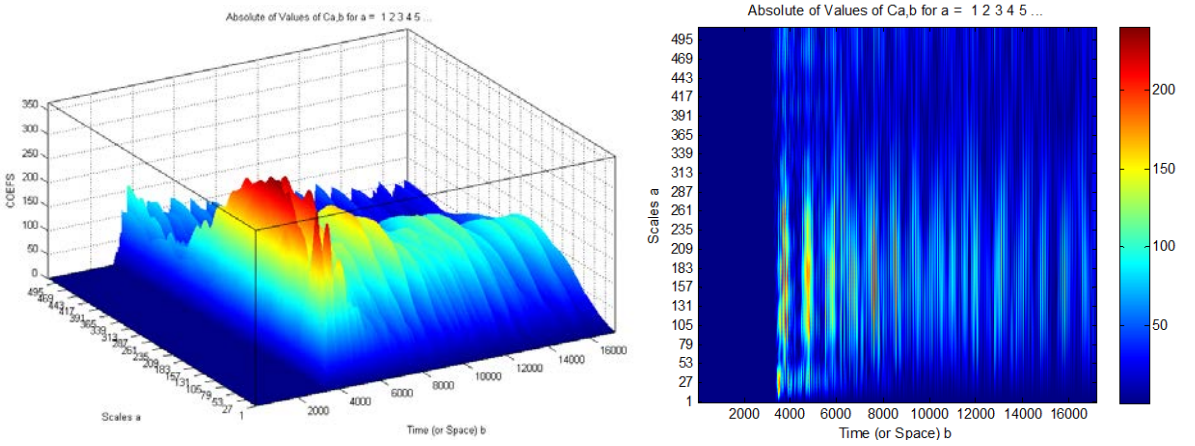

(a)

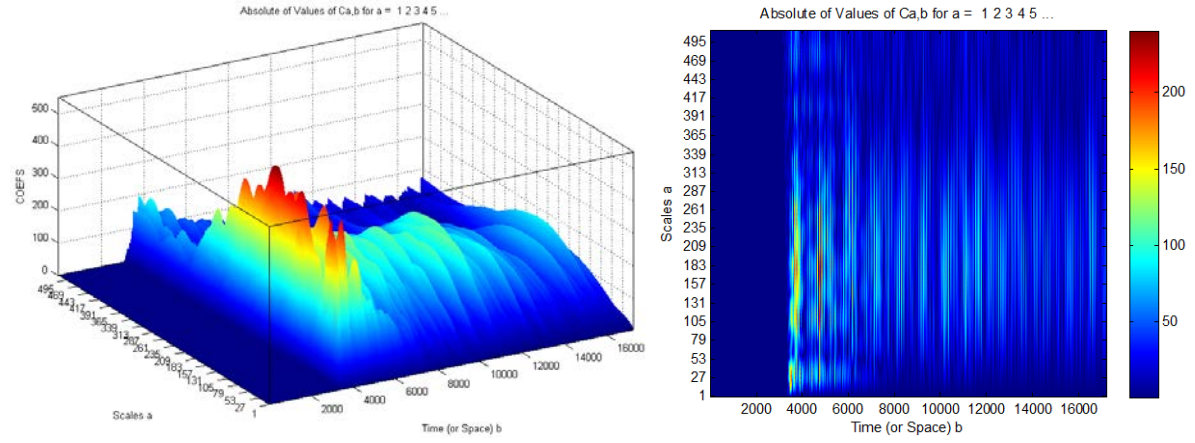

(b)

Figure 10: Continuous wavelet analysis results of (a) the reference and (b) the modified structure. (Remark: time labels do not represent physical unit, but the number of samples)

It should be noted that there is a difference in the magnitude of scales for the reference and the modified structure. In the modified structure, the frequencies are more clearly separated from each other. Another observation is that the magnitude of the frequencies is higher for the modified structure than for the reference one.

5 CONCLUSIONS

This work presents an experimental case study of a frame structure, aimed at diagnosis of the state of its bolted connection. To this end, classical experimental modal analyses were performed for the reference (Test I) and modified (Test II) structures. All bolted connections of the reference structure are rigid, whereas in the modified structure two of two bolts from a selected connection are removed. Modal parameters were determined using 20 uniformly distributed accelerometers collecting signals induced by a modal hammer.

The localization of the damaged bolted connection is performed using perturbation of the modal shapes, obtained experimentally for the reference and modified structure. The procedure is based on the Damage Connection Index, which utilizes the differences in rotation angles calculated at the bolted connections for an individual mode shape.

Generally, one can conclude that the FRFs determined for the reference and modified structures overlap in the frequency range from 0 to 400 Hz. The introduced structural modification produces some perturbations in the narrow band of the frequency. The final observation is that only 3 out of 17 mode shapes and corresponding frequencies reveal measurable differences.

A wavelet analysis of the output signal of both structures shows that there is some difference between those two signals. The wavelet representation gives a qualitative index which helps to conclude the damage. As a next step, a procedure for quantifying the damage should be developed.

ACKNOWLEDGEMENTS

The two first authors are grateful for financial support from the National Science Centre of Poland (grant N N501 0494 40).

REFERENCES

[1] A. Świercz, P. Kołakowski, J. Holnicki-Szulc, Structural damage identification using low frequency non-resonance harmonic excitation, *Key Engineering Materials*, **347**, 427-432, 2007.

[2] A. Świercz, P. Kołakowski, J. Holnicki-Szulc, Impulse Virtual Distortion Method for Single Damage Identification in Structures, *Proc. of the 16th International Conference on Computer Methods in Mechanics - CMM'05*, 2005.

[3] S. Caddemi, A. Morassi, Multi-cracked Euler-Bernoulli beams: Mathematical modeling and exact solutions, *International journal of solids and structures*, **50(6)**, 944-956, 2013.

[4] S. Caddemi, A. Morassi, Crack detection in elastic beams by static measurements, *International journal of solids and structures*, **44(16)**, 5301-5315, 2007.

[5] A. Zak, M. Krawczuk, W. Ostachowicz, Elastic wave propagation in a cracked isotropic plate, *Proceedings of the 3rd European Workshop Structural Health Monitoring*, 316-323, 2006.

[6] M. Krawczuk, M Palacz, W Ostachowicz, Wave propagation in plate structures for crack detection, *Finite elements in analysis and design*, **40(9-10)**, 991-1004, 2004.

[7] J. Yang, Y. Xia, and C. Loh, Damage Identification of Bolt Connections in a Steel Frame. *Journal of Structural Engineering*, **140(3)**, 2014.

[8] M. Mehrjoo, N. Khaji, H. Moharrami, A. Bahreininejad, Damage detection of truss bridge joints using Artificial Neural Networks, *Expert Systems with Applications*, **35(3)**, 1122-1131, 2008.

[9] B. Blachowski, W. Gutkowski, Revised assumptions for monitoring and control of 3D lattice structures, *Proceedings of the 11th Pan-American Congress of Applied Mechanics PACAM XI*, Foz do Iguassu, Brasil, 4-8 January 2010.

[10] P. Razi, R.A. Esmaeel, F. Taheri, Improvement of a vibration-based damage detection approach for health monitoring of bolted flange joints in pipelines, *Structural Health Monitoring*, **12 (3)**, 207-224, 2013.

[11] W.J. Staszewski, Structural and mechanical damage detection using wavelets, *Shock Vibration Digest*, **30(6)**, 457–472, 1998.

[12] D.E. Newland, *An introduction to random vibrations, spectral and wavelet analysis.* Longman Singapore Publishers (Pte) Ltd, 1993.

[13] N.G. Pnevmatikos, Damage detection of structures using discrete wavelet transform, *Fifth World Conference on Structural Control and Monitoring (5WCSCM)*, Tokyo, Japan, 12-14 July 2010.